

Supporting Information to the paper

From Dense Monomer Salt Crystals to CO₂ Selective Microporous Polyimides via Solid-State Polymerization

by

Miriam M. Unterlass*, Franziska Emmerling, Markus Antonietti and Jens Weber.

1	Experimental details	2
1.1	Synthesis of monomer salts	2
1.2	Solid-State polymerizations of monomer salts	2
2	Characterization of monomer salts and PIs	2
2.1	Room-temperature powder X-Ray diffraction of monomer salts	2
	<i>Fig.S1: Powder XRD diffractograms of monomer salts under ambient conditions</i>	3
2.2	Crystal Structure determination of 3a	3
	<i>Fig.S2: Structure of (S)-PMA-H₂BAPF</i>	4
2.3	Analytical Ultracentrifugation	4
	<i>Fig.S3: AUC density gradient analysis of monomer salts</i>	5
2.4	FT-IR-ATR analyses of monomer salts and polymers	5
	<i>Fig.S4: FT-IR spectra of monomer salts and corresponding polyimides</i>	5
2.5	Buoyancy measurements of polyimide 4a	6
2.6	Size Exclusion chromatographic determination of the molecular weight distribution	6
	<i>Fig.S5: Size Exclusion Chromatogramm and MWD of 4a.</i>	7
2.7	High-temperature in-situ synchrotron XRD of solid-state polymerizations	7
	<i>Fig.S6: HT-XRD monitoring of the transformations from monomer salt to polymer for both studied systems.</i>	8
2.8	Scanning electron microscopy	8
	<i>Fig.S7: SEM images of monomer salt 3b prior to SSP and corresponding polyimide 4b after polymerization.</i>	8
3	Gas adsorption measurements and analysis	8
3.1	Single gas adsorption measurements and fits	8
	<i>TableS1: Fit parameters obtained from the Langmuir or dual-site approach.</i>	9
	<i>Fig.S8: Adsorption/Desorption isotherms of PIs and fits at 273.15K</i>	10
	<i>Fig.S9: Adsorption/Desorption isotherms of 4a and fits at 298.25K.</i>	10
3.2	IAST calculations	11
	<i>Fig.S10: IAST selectivity and predicted uptakes from a CO₂/N₂ gas mixture.</i>	11
3.3	Initial Gas Breakthrough Experiments	11
	<i>Fig.S11: Exemplary breakthrough curves of N₂ and CO₂</i>	12
	<i>Fig.S12: Flow scheme of the used breakthrough device.</i>	12

1. Experimental details

1.1. Synthesis of monomer salts

9,9'-Bis(4-aminophenyl) fluorine (BAPF, **1**), 99%, was purchased from Aldrich and recrystallized from analytical grade ethanol. Pyromellitic dianhydride (PMDA, **2a**), 97%, was purchased from Aldrich and either used as received or recrystallized from freshly distilled acetic anhydride. 3,3',4,4'-Biphenyltetracarboxylic acid dianhydride (BPDA, **2b**), 99%, was purchased from AK Scientific, Inc., 99% and equally either used as received or recrystallized from freshly distilled acetic anhydride. Monomer salts **3a** and **3b** were prepared according to a previously described procedure (M. M. Untrelass *et al. Polym. Chem.* **2011**, 2, 1744; Ref. [9]). **3a**: 1.5mmol of **2a** were dissolved in 10mL of deionized water by stirring for 2h at 70°C. PMDA gets thereby hydrolyzed to PMA and a clear colourless solution is obtained. 1.5mmol of **1** were then added to that solution, and the mixture was kept at the same temperature for another 2 h. The final white precipitate was filtered and washed with deionized water. The white solid was collected and dried *in vacuo* at 40°C for 12 hours. **3b**: The same procedure was applied for synthesizing **3b**. **2b** does not entirely dissolve in hot water, but upon addition of **1**, the dissolved part of **2b** gets consumed to form the salt and thus further dissolution of **2b** takes places. After 2h of stirring, **3b** is obtained quantitatively as white precipitate, and no residues of **1** or **2b** are observed.

1.2. Solid-state polymerizations of monomer salts

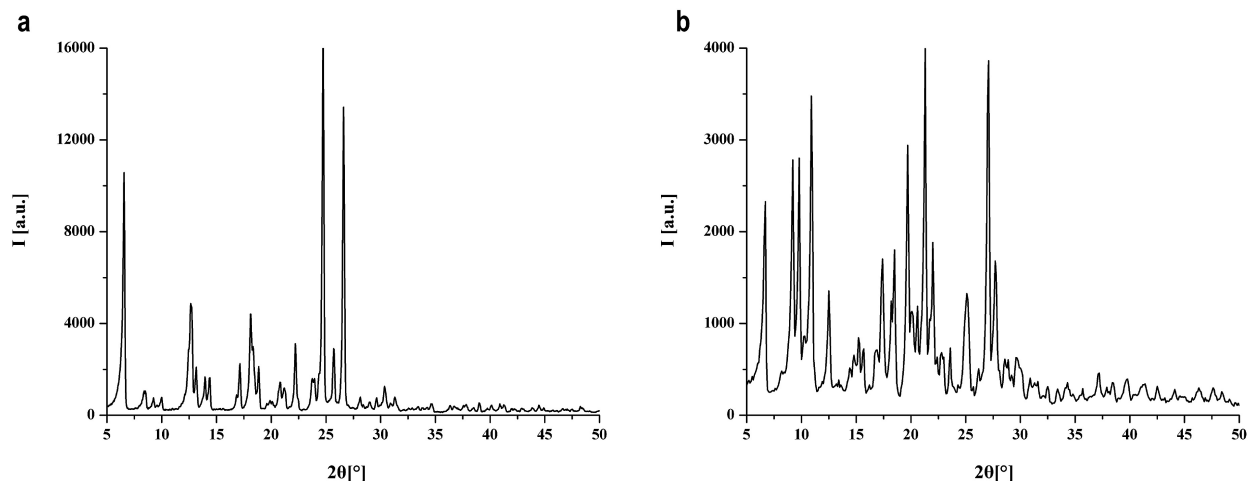
0.281g of thoroughly dried monomer salt PMA-H₂BAPF (**3a**) was placed in a dry flask. The flask was placed in a heating mantle and heated up to 270°C for 2 hours. It was kept at this temperature for three hours and then allowed to slowly cool down to RT. 0.244g of a yellow-orange solid was obtained. *Y* = 98.5%. The same procedure applied for BPCTA-H₂BAPF (**3b**), with the only difference being the polymerization temperature of 250°C for **3b**.

2. Characterization of monomer salts and polyimides

2.1. Room-temperature powder X-ray diffraction of monomer salts

RT XRD measurements were performed with a *D8 Advance* machine from *Bruker Instruments*. The radiation was of the wavelength of CuK α (0.154 nm). Measurements were undertaken in reflection geometry. Samples were measured as fine powders on a silicon sample holder.

Fig.S1. Powder XRD diffractograms of monomer salts under ambient conditions. a) **3a** (PMA-H₂BAPF). b) **3b** (BPCTA-H₂BAPF). a,b) Intensity in arbitrary units is plotted vs. scattering angle 2θ in $^{\circ}$.

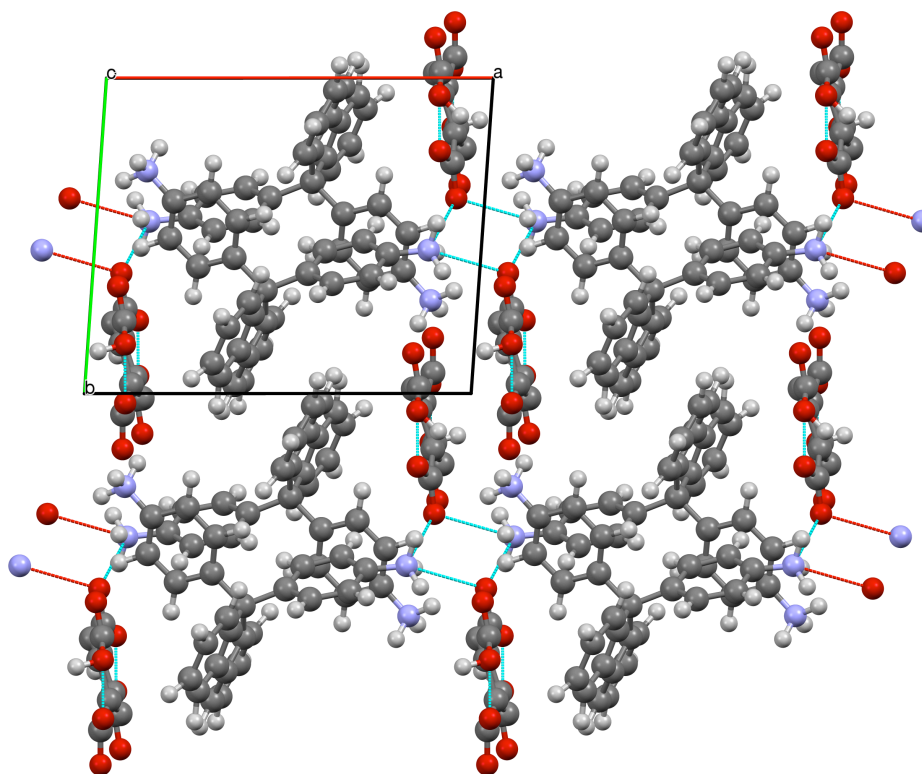


2.2. Crystal Structure determination of **3a**

In order to perform structure determination from PXRD, a high-quality diffractogram obtained from a measurement in transmission geometry was necessary. Therefore, **3a** had to be measured again (see Fig.2a (in the paper) for observed pattern) XRD ambient conditions: Powder pattern was collected using a *Bruker D8 Discover* (Bruker AXS GmbH, Germany) operated in transmission geometry and equipped with a SolX detector. The samples were measured over a range of 5-70° 2θ (2 kW; Cu-Kα, 1.54056 Å, step width 0.009° 2θ, count time 20 s/step).

The structure determination of **3a** was achieved using the open source program FOX (Favre-Nicolin, V.; Cerny, R. *J. Appl. Cryst.* **2002**, 35, 734. Ref. [15]). FOX uses global-optimization algorithms that perform trials in direct space. This search algorithm employs random sampling coupled with Monte Carlo simulated temperature annealing (MC/SA) to locate the global minimum of the figure-of-merit factor. Phenyl rings were refined as a rigid group in order to reduce the total number of degrees of freedom. The crystal structure of **3a** was solved by the simulated annealing procedure on a standard personal computer within 4 hours, finding the deepest minimum of the cost function several times during the procedure. To complete the structure determination, the structural solution obtained from simulated annealing was subsequently subjected to a Rietveld refinement employing the TOPAS software (Topas Version 4.2, General Profile and Structure Analysis Software for Powder Diffraction Data (2009) Bruker AXS, Karlsruhe (Germany)). The refinement converged to $R_{wp} = 5.873\%$ ($R_{Bragg} = 4.658\%$). Unit cell parameter for **3a**: triclinic, P-1, $a = 13.3709(20)$ Å, $b = 11.5729(19)$ Å, $c = 10.4381(17)$ Å, $\alpha = 111.3395(60)^\circ$, $\beta = 99.9454(69)^\circ$, $\gamma = 90.0923(59)^\circ$, $V = 1478.18(41)$ Å³. **CCDC-955505** contains the supplementary crystallographic data for (S)-PMA-H₂BAPF. The data can be obtained free of charge from the Cambridge Crystallographic Data Centre via www.cdc.cam.ac.uk/data_request/cif.

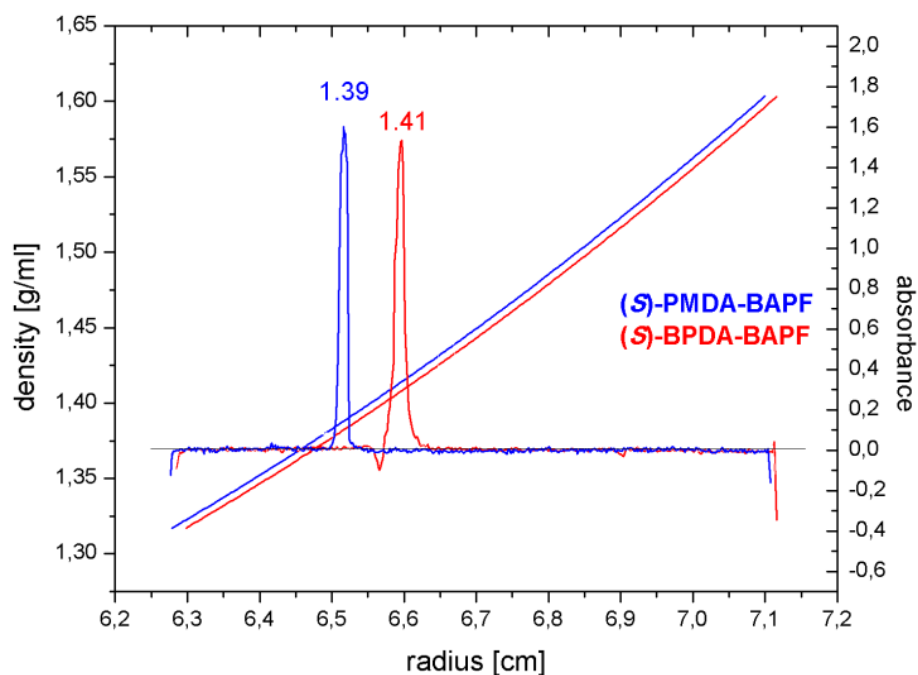
Fig.S2. Structure of (S)-PMA-H₂BAPF: Obtained from Rietveld refinement and MC/SA of powder XRD data, view along c-axis. Grey: carbon atoms, white: hydrogen atoms, blue: nitrogen atoms, red: oxygen atoms; blue dotted lines: hydrogen-bonding.



2.3. Analytical ultracentrifugation density gradient analysis of monomer salts

AUC was carried out with an *Optima XL-I* ultracentrifuge (*Beckmann-Coulter, Palo Alto, CA*). An absorption optics detection system ($\lambda=400\text{nm}$) was used. The ultracentrifuge was operated at 40000 rpm, at RT. Data analyses were carried out with the program NewGradient (*Kristian Schilling, Nanolytics, Germany*).

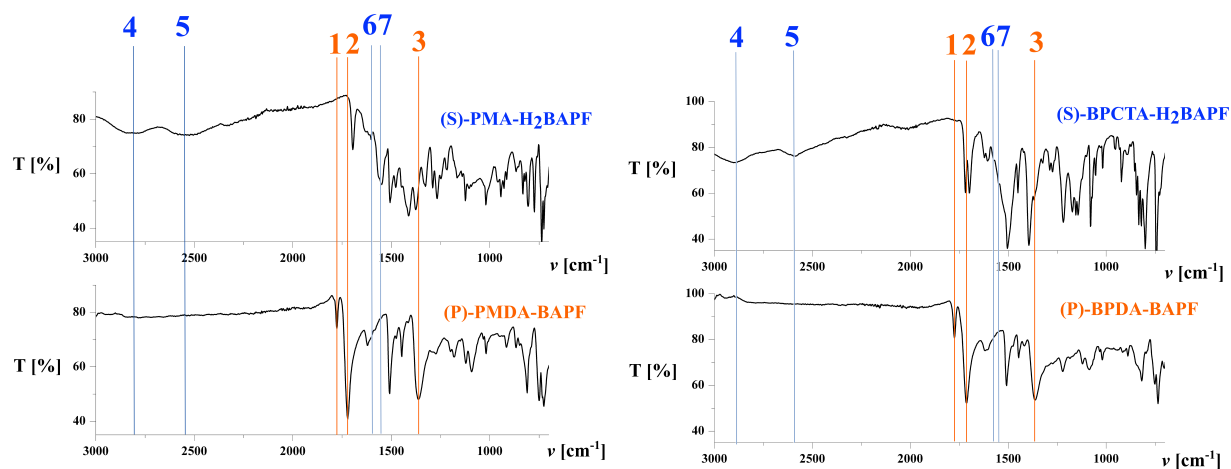
Fig.S3. AUC density gradient analysis of monomer salts: The absorption peak of each salt can be attributed to its corresponding calculated density by the density distribution of the pure solvent mixture (quasi-linear lines). Cell radius in [cm] is plotted vs. absorbance ([dimensionless], right ordinate) and the corresponding density (in [g/mL], left ordinate). A solvent mixture of toluene : bromoform with ratio 0.71:0.29 was used. The near-linear lines show the density evolution of the pure solvent mixture during ultra- centrifugation. The blue (**3a**, (S)-PMA-H₂BAPF) and red (**3b**, (S)-BPTCA-H₂BAPF) peaks are the absorbance signal of the cells containing a dispersion of the corresponding monomer salt. The density of each salt is determined by using the radii-vs.-absorbance plot of the pure solvent mixture as calibration curve. All measurements were carried out twice for certainty.



2.4 FT-IR-ATR analyses of monomer salts and polymers

FT-IR spectra of dry powders of **3a**, **3b**, **4a** and **4b**, respectively, were collected with a *Varian 1000 FT-IR (scimitar series)* spectrometer, equipped with an attenuated total reflection (ATR) setup.

Fig.S4. FT-IR spectra of monomer salts and corresponding polyimides. Left side: PMDA-BAPF system; top: (S)-PMA-H₂BAPF (**3a**), bottom: (P)-PMDA-BAPF (**4a**). Right side: BPDA-BAPF system; top: (S)-BPCTA-H₂BAPF (**3b**), bottom: (P)-BPDA-BAPF (**4b**). For both systems the classical imide modes (1,2,3 - orange) appear in the spectrum of the polymeric product. 1 \approx 1775cm⁻¹: asymmetric carbonyl vibration mode of the cyclic imide; 2 \approx 1720cm⁻¹: symmetric carbonyl vibration mode of the cyclic imide; 3 \approx 1365cm⁻¹: C-N symmetric stretching mode of the cyclic imide. Moreover, in both cases, the salt bands (4,5,6,7 - blue) disappear. 4, 5 \approx 2580cm⁻¹, 2830cm⁻¹: asymmetric and symmetric aryl-amminium modes; 6,7 \approx 1605, 1570cm⁻¹: asymmetric and symmetric carboxylate modes.



2.5 Buoyancy measurements of polyimide 4a

The density of **4a** was determined via buoyancy measurements of the solid powder in water using the IMETER® method. The determination of the density of a solid sample with this technique uses hydrostatic weighing: the sample immersed in a fluid seems lighter by the weight of the volume of the fluid it displaces (Archimedes' principle). In order to determine the density of the solid body from the buoyancy force, one needs to determine the volume and the mass of the solid body as a function of both temperature and pressure. In addition, the density of the medium in which the solid body is weighed (here air) has to be taken into account. Measurements were carried out by Michael Breitwieser of IMETER®, Germany.

Prior to measuring the density of **4a**, the measurement fluid's (deionized water) density was determined to be $\rho_{l,25^\circ\text{C}} = 0,997047 \text{ g cm}^{-3}$, with a thermal expansion coefficient $\kappa = -21.93 \cdot 10^{-5} \text{ K}^{-1}$. The density of the solid powder of **4a** was determined at a measurement temperature of 21°C according to the following formula:

$$\rho_s = \frac{(\rho_l - \rho_{\text{air}})}{1 + \frac{W_{V,l} - W_{V,l+s}}{W_s}} + \rho_{\text{air}} \quad (\text{Eq.S1})$$

with ρ_s = density of the solid sample, ρ_l = density of the fluid, ρ_{air} = density of air, $W_{V,l}$ = mass of the pycnometer filled completely with the fluid, $W_{V,l+s}$ = mass of the pycnometer with the solid sample and then filled to completion with the fluid, W_s = mass of the solid sample.

The following values were obtained:

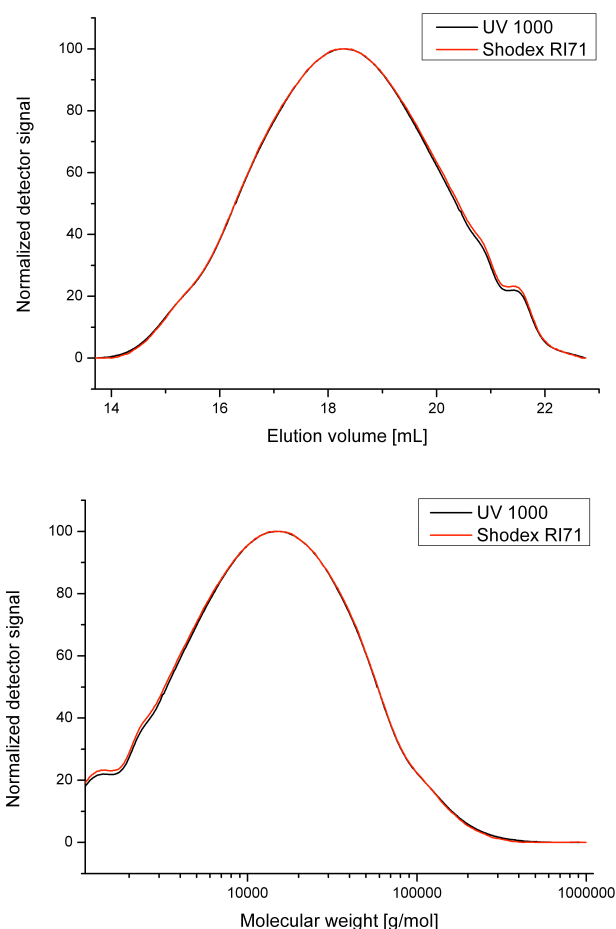
$$\begin{aligned} W_{V,l} &= 75.7804 \text{ g} \\ W_{V,l+s} &= 75.9495 \text{ g} \\ W_s &= 0.7806 \text{ g} \\ \rho_{\text{air}} &= 0.0011234 \text{ g cm}^{-3} \\ \rho_{l,21^\circ\text{C}} &= 0.9980 \text{ g cm}^{-3} \end{aligned}$$

Thus resulting in $\rho_s = 1.274 \text{ g cm}^{-3}$ according to Eq.1 for **4a**.

2.6 Size Exclusion chromatographic determination of the molecular weight distribution

Size Exclusion Chromatography (SEC) in 0.05 mol L^{-1} LiBr in NMP as the eluent and methyl benzoate as internal standard was performed with a system from *Thermo Separation Products* containing PSS GRAM 100 Å/1000 Å to 7 mm (particle size) columns from *PSS-Polymer Standards Service*. GRAM is a polyester column material without reactive functional groups. The column dimensions are of 8x50 mm for the pre-column and 8x300 mm for the main columns, respectively. It provides simultaneous UV and RI detection. 100 mL of sample with a concentration of 1.5 g L^{-1} were injected and separated at 70°C and a flow of 0.8 mL min^{-1} . Samples were filtered through 0.45 mm syringe filters prior to use. Polystyrene calibration standards of different molecular weights from *PSS-Polymer Systems Service* were used. Data treatment was performed with the software package *NTeqGPCv6.4* from *hs GmbH*.

Fig.S5. Size Exclusion Chromatogramm and MWD of 4a. Normalized detector signal is plotted vs. elution volume in mL (top) and MWD plotted as normalized detector signal vs. molecular weight in g/mol (bottom). Detector signals of the UV (black line) and the RI (red line) detector correspond well. The weight average molecular weights obtained from universal calibration are of $\overline{M}_w(\text{UV}) \approx 22500 \text{ g/mol}$ and $\overline{M}_w(\text{RI}) \approx 22100 \text{ g/mol}$, from the respective detector signals, with corresponding polydispersity indices of $\text{DI}(\text{UV}) \approx 3.72$ and $\text{DI}(\text{RI}) \approx 3.71$.

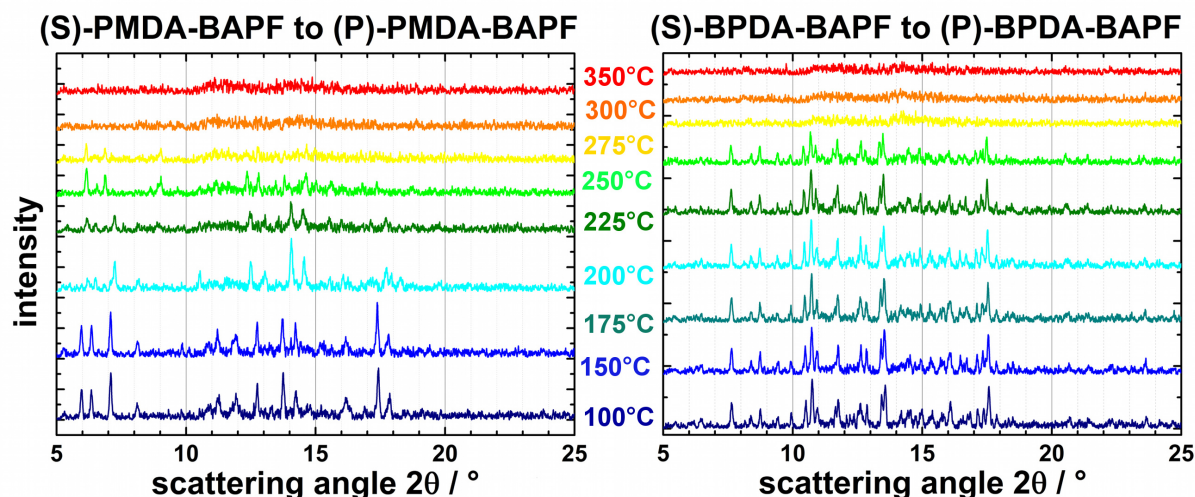


2.7 High-temperature in-situ synchrotron XRD of solid-state polymerizations

HT-XRD was conducted at the B2 Beamline (DORIS III) of Hasylab/DESY using X-rays of energy of 12.4 keV. The salts were filled in suitable capillaries (0.5 mm diameter) and heated under ambient atmosphere.

The recorded patterns are depicted in Fig.S6. In both cases we find a transition from highly crystalline salts to amorphous products. For (S)-PMA-H₂BAPF a high-temperature intermediate occurs at 200°C (light blue in Fig.S6), whereas no such intermediate is detectable for (S)-BPCTA-H₂BAPF.

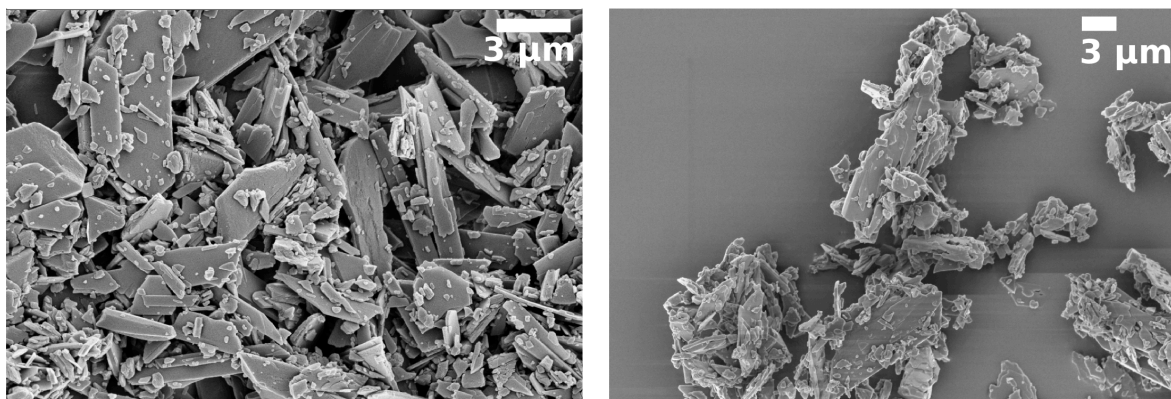
Fig.S6. HT-XRD monitoring of the transformations from monomer salt to polymer for both studied systems. Intensity (in arbitrary units) is plotted vs. scattering angle 2θ in °. Left side: transformation of monomer salt **3a** to polymer **4a**. Right side: transformation of monomer salt **3b** to polymer **4b**.



2.8 Scanning electron microscopy

SEM images were collected with a *Gemini Leo 1550* microscope at 3 kV. The samples were loaded on carbon coated stubs and coated by sputtering with Au/Pd alloy prior to imaging.

Fig.S7: SEM images of monomer salt 3b prior to SSP and corresponding polyimide 4b after polymerization. Left side: (S)-BPCTA- H_2 BAPF (**3b**); right side: (P)-BPDA-BAPF (**4b**). scale bar is 3 micron in both images.



3. Gas Adsorption Measurements and Analysis

3.1 Single gas adsorption measurements

Gas adsorption experiments were performed with an *Autosorb-1 MP* (*Quantachrome Instruments*) machine. Temperature of 273.15 K was established using a thermostated water/ethylene glycol mixture. Initial data analysis was performed using either *ASiWin* or the *Quadrasorb 5.05* software package (*Quantachrome Instruments*). Measurements are conducted using an equilibration time setting of 3 min (the time interval, in which the pressure change must be below the allowed difference, typically $\Delta p < 0.0008$ atm). An equilibration time of 3 min is a commonly used “default” value of the *Autosorb-1* machine of *Quantachrome Instruments*.

High-purity gases were used throughout the experiments. Samples were degassed using the built-in outgasser of the *Autosorb-I MP* machine (turbomolecular vacuum pump) at 150°C for at least 20 hours before analysis.

The gas adsorption isotherms were fitted using either a simple Langmuir approach (CO₂, N₂, Eq.S2) or a dual-site Langmuir approach (CO₂, Eq.S3)

$$q = \frac{(q_{\max} \cdot a \cdot p)}{(1 + a \cdot p)} \quad (\text{Eq. S2})$$

$$q = \frac{(q_{\max} \cdot a \cdot p)}{(1 + a \cdot p)} + \frac{(u_{\max} \cdot b \cdot p)}{(1 + b \cdot p)} \quad (\text{Eq. S3})$$

p : pressure of the bulk gas at equilibrium with the adsorbed phase in mmHg, q : adsorbed amount in [cm³/g STP], q_{\max} , u_{\max} : saturation capacities in [cm³/g STP], a, b affinity coefficients in [1/mmHg]

Table S1. Fit parameters obtained from the Langmuir or dual-site approach.

	q [cm ³ /g STP]	u [cm ³ /g STP]	a [1/mmHg]	b [1/mmHg]
(P)-PMDA-BAPF (4a)				
N ₂ , 273 K (Langmuir)	1.65003		0.0025	
CO ₂ , 273 K (dual-site)	12.28903	42.80565	0.01297	7.02583E-4
CO ₂ , 273 K (Langmuir)	35.08592		0.0034	
N ₂ , 298 K (Langmuir)	2.099832		0.000825	
CO ₂ , 298 K (dual-site)	7.505544	37.848289	0.006353	0.000653
(P)-BPDA-BAPF (4b)				
N ₂ , 273 K (Langmuir)	2.39466		0.00103	
CO ₂ , 273 K (dual-site)	10.35173	39.8029	0.01495	8.71693E-4
CO ₂ , 273 K (Langmuir)	34.39787		0.00334	

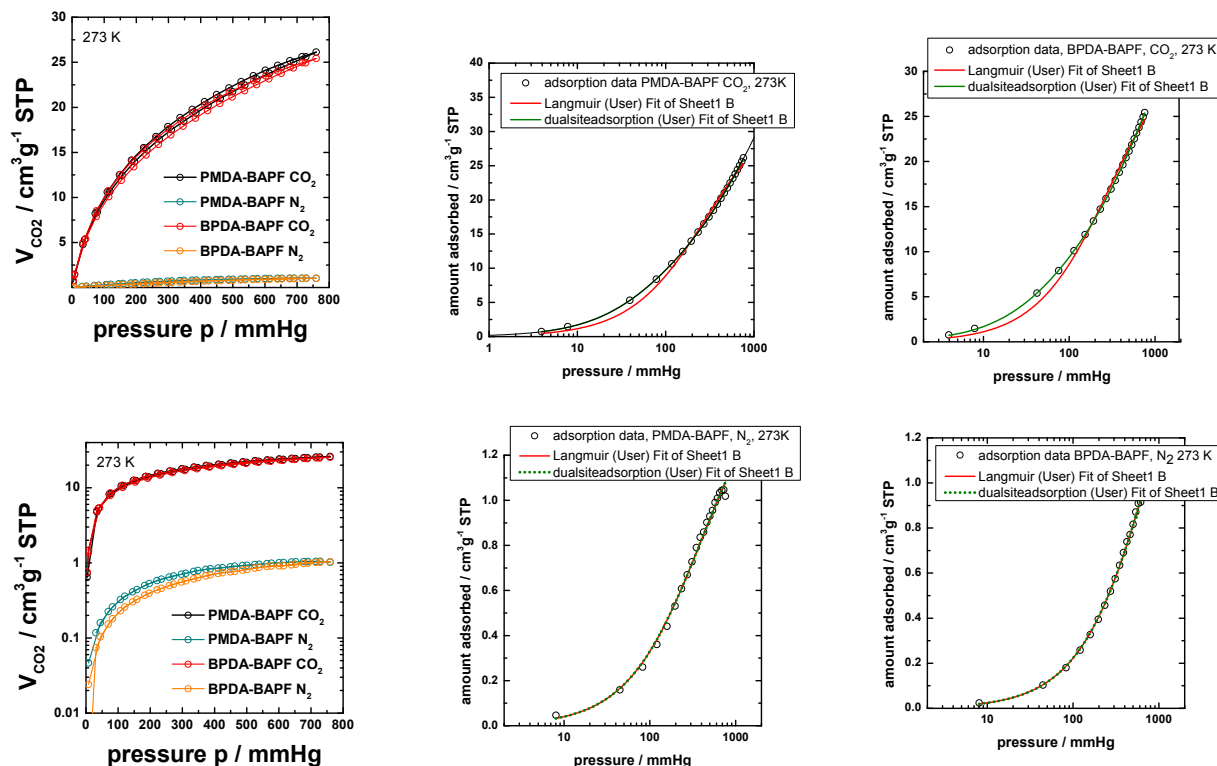


Fig.S8: Adsorption/Desorption isotherms of PIs and fits at 273.15K. Left side: adsorption/desorption isotherms of the polyimides obtained at 273.15 K in linear scale (upper left) and log-scale (lower left); middle-panels and right panels show fit quality, upper panels: CO₂; lower panels N₂.

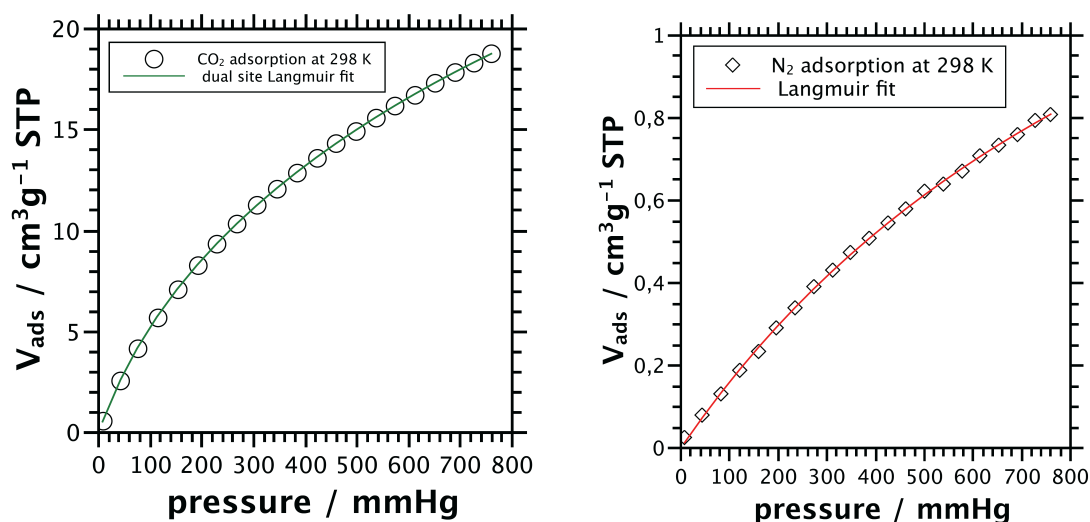


Fig.S9: Adsorption/Desorption isotherms of 4a and fits at 298.25K. left side: CO₂ adsorption/desorption isotherm and its dual-site Langmuir fit of (P)-PMDA-BAPF at 298.15 K; right side: N₂ adsorption/desorption isotherm and its Langmuir fit of (P)-PMDA-BAPF at 298.15 K.

3.2 IAST calculations

Selectivity was calculated using the common IAST equation S4¹:

$$\alpha(\text{CO}_2 / \text{N}_2) = \frac{x_{\text{CO}_2} / x_{\text{N}_2}}{y_{\text{CO}_2} / y_{\text{N}_2}} \quad (\text{Eq.S4})$$

where α is the selectivity, x the adsorbed amount and y represents the gas phase composition.

x_{CO_2} was determined using a Newton-Raphson method implemented within a *MatLab*® (*R2011a*) script or an *octave* (open source software) script, these scripts are available for download at: <http://www.mpikg.mpg.de/144866/xDownloads> or upon request via e-mail. The amount adsorbed from the mixed-gas phase was also determined following the known protocols based on Ref. (1) using the above shown fit parameters as basis for the analytical description of the single-gas adsorption isotherms. The gas phase composition was set 15 vol.-% CO_2 and 85 vol.-% N_2 , *i.e.* $y_{\text{CO}_2} = 0.15$ and $y_{\text{N}_2} = 0.85$

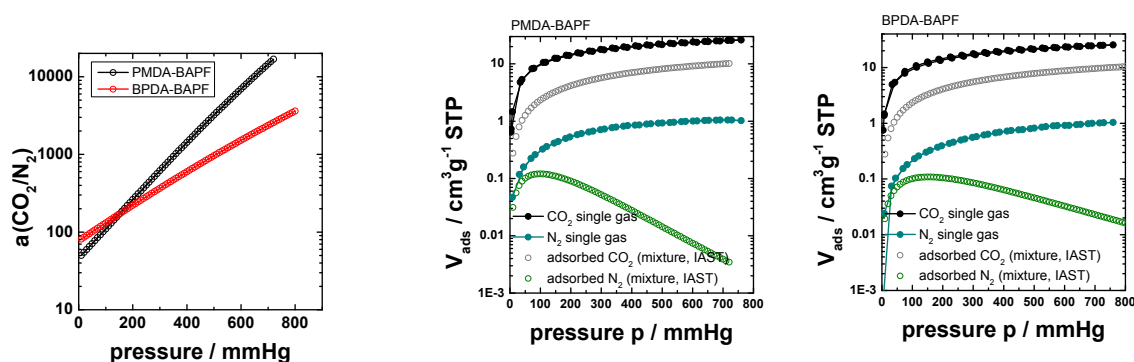


Fig.S10. IAST selectivity and predicted uptakes from a CO_2/N_2 gas mixture. *left side:* IAST selectivity of (P)-PMDA-BAPF (**4a**) and (P)-BPDA-BAPF (**4b**) for a gas mixture (0.15/0.85 of CO_2/N_2) at 273.15 K; *middle panel and right side:* experimental single gas adsorption isotherms of CO_2 and N_2 on (P)-PMDA-BAPF and (P)-BPDA-BAPF, respectively, together with predicted uptakes from a 0.15/0.85 gas mixture of CO_2/N_2

3.3 Initial Gas Breakthrough Experiments

In order to see, whether the material can indeed separate CO_2 from N_2 , initial breakthrough experiments were performed using a custom setup (see below for flow scheme). 0.9g of (P)-PMDA-BAPF were filled in a stainless steel column of 7 mm inner diameter and 100 mm length and degassed by He purge. The column was closed by glass wool and connected to a gas stream. A mass spectrometer (*ThermoStar*™ *DSD 301 T2*) was connected to the outlet gas flow to monitor gas concentrations qualitatively. CO_2 and N_2 were premixed at ratios between $\sim 1:1$ and $\sim 0.5:1$ and a total gas flow of roughly 0.15 L/min was used. A slight backpressure of 0.3-0.5 bar was generated typically.

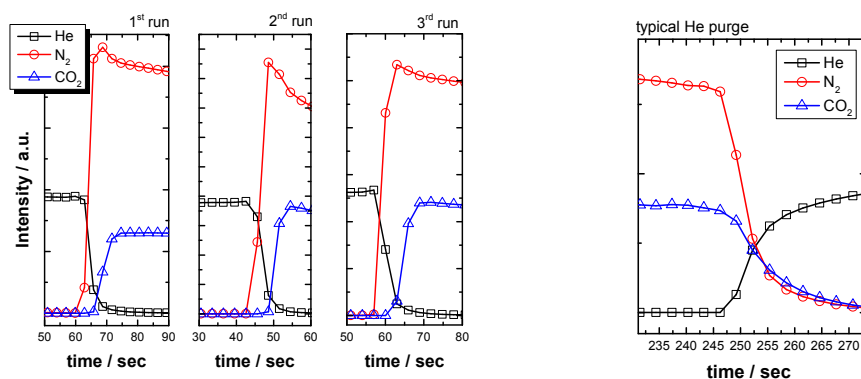


Fig.S11: Exemplary breakthrough curves of N_2 and CO_2 . N_2 (red) and CO_2 (blue) at 298 K using (P)-PMDA-BAPF (**4a**) as adsorber, please note the baseline separation in all cases. *right side:* typical concentration patterns upon He purge, the slope of the CO_2 decay is typically lower, indicating stronger retention.

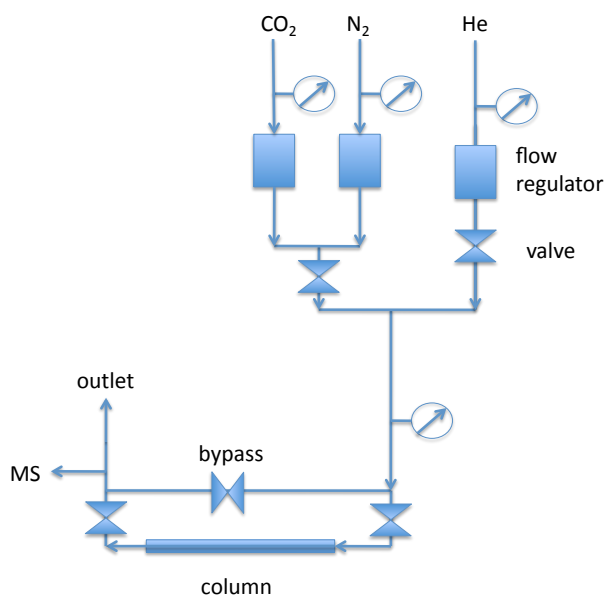


Fig.S12: flow scheme of the used breakthrough device.

(S1) Myers, A. L.; Prausnitz, J. M. *AIChE Journal* **1965**, *11*, 121–127.